ICRANET2018-180141

ENVIRONMENTALLY BENIGN CATALYTIC CONVERSION OF WASTE COOKING OIL INTO BIODIESEL USING IRON IMPREGNATED ACTIVATED CARBON

Irfan Shah*
Chemistry Section
University of Agriculture, Faisalabad
Sub Campus Toba Tek Singh
irfan.shahg2015@gmail.com

Rohana Adnan
School of Chemical Sciences
Universiti Sains Malaysia
11800 Penang, Malaysia
r_adnan@usm.my

Haq Nawaz Bhatti
Department of Chemistry
University of Agriculture
Faisalabad
hnbhatti2005@yahoo.com

Umar Farooq
University of Agriculture
Faisalabad,
Sub Campus Toba Tek Singh
u.farooq@uaf.edu.pk

Muhammad Ashraf
Institute of Animal and Dairy Sciences
University of Agriculture
Faisalabad
professorashraf@uaf.edu.pk

Abstract

A renewable energy approach using waste feedstock i.e. waste cooking oil (WCO) to produce biodiesel using a series of iron impregnated activated carbon materials (FeACs) as reusable heterogeneous catalysts is reported. The morphological examination of FeACs was conducted via scanning electron microscopy, transmission electron microscopy, high resolution transmission electron microscopy and selected area electron diffraction analyses. Moreover, temperature programmed reduction (TPR-H_2) and temperature programmed desorption (TPD-CO_2) techniques were used to evaluate the strength of acidic and basic sites on the FeACs which were accountable for the catalytic characteristics of the materials. The catalytic potential of FeACs was described by the TPR/TPD results along with the biodiesel produced from WCO in a cost effective pathway. The iron impregnated AC catalyst having composition 1 M : 1 M molar ratio of $KMnO_4$ to $FeSO_4.7H_2O$, showed the highest fatty acids methyl ester (FAME) yield of 78% under mild reaction conditions i.e. 120° C and the reaction time of 5 h. This character adds more values to the otherwise inert AC and is crucial from energy and environmental perspectives.

Keywords: biodiesel; catalysis; impregnation; carbon.

1. INTRODUCTION

Activated carbon (AC) is well known adsorbent material for the removal of organic and inorganic pollutants from the aqueous media. Its surface chemistry plays a crucial role in removing pollutants from water. Although, the various applications of AC are well described but the treatment of ACs surface during preparation and afterwards shed more light on the diverse and extended applications of the same material. Yin et al., [1] thoroughly described the enhanced efficiency of AC via surface modifications. The physical, chemical and biological treatments are usually adapted to tailor the AC surface. In general, surface characteristics of the substrate (AC) can be upgraded as per required application.

The extensive use of fossil fuels, global warming and shortage of energy resources urged researchers to explore alternate energy sources. In this connection, biodiesel has been defined as clean burning fuel having low quantity of sulphur and aromatics contents, high cetane number and lubricity, and also is helpful in reducing greenhouse gases emission [2]. The other advantageous aspects of biodiesel are biodegradability, environmentally friendly, renewability and can be used as such in the conventional ignition engines without requiring any specific setup of the existing engines [3]. The catalytic transesterification of oils (edible or non-edible) in the presence of alcohol produces fatty acid methyl ester (FAME) referred to as biodiesel along with a bye-product glycerin [4].

2. ACTIVATED CARBON AS CATALYST

In addition to the adsorbent character of AC, its catalytic potential in the presence of metals, non-

stoichiometric oxides and acids are well described elsewhere [5]. It is pertinent to mention that, sulfonated carbon-based catalysts have been proposed as economical and renewable "green catalysts" and has been used as support material for the sulfonic groups (–SO_3H) [6]. Recently reported works on sulfonated carbon materials as solid catalysts have shown some promising results [7]. Moreover, the sulfonated-carbon catalysts are expected to be the alternative solid acid catalysts for homogeneous catalyst (e.g. H_2SO_4) in catalytic esterification reactions of glycerol [6]. The Conventional homogeneous acids/bases catalysts such as H_2SO_4, NaOH, KOH, CH_3ONa, $Fe_2(SO_4)_3$ etc. have been effectively applied for the production of biodiesel. However, the corrosive nature of acid catalysts, non-reusability, monotonous separation from the mixture due to their high solubility, side reactions, and environmental pollution (excess water use for washing) limit the use of homogeneous catalysts on large scale production of biodiesel [8]. Ultimately, the operational cost increases.

In comparison, heterogeneous catalytic transesterification produces biodiesel in a cost effective manner due to the reusability of the catalyst, immiscibility with the reaction mixture, easy separation thus avoiding extensive water use which is crucial for environmental protection and water control. Generally, heterogeneous catalysts are expected to have large pore size, high acidic sites and stability, hydrophobic surface, high adsorption affinity and repulsion of highly polar compounds [9].

3. CHEMICAL REAGENTS AND METHODOLOGY

3.1 Chemical Reagents

All chemical reagents used were of analytical grade. The AC characteristics have been depicted in Appendix A. The chemicals were arranged from various sources as follows; AC from R & M Chemicals (UK), $KMnO_4$ from Amresco (USA), the metal precursor, $FeSO_4.7H_2O$ and $NaHCO_3$ from ACROS Organics (USA), methanol from John Collin Corporation (USA), KBr for FTIR and standards for GC analyses were provided by Sigma-Aldrich (USA). The carrier gases CO_2 and He were obtained from Malaysian Oxygen Berhad.

3.2 Iron impregnated ACs preparation

The substrate AC was dried in oven to remove any moisture contents. It was reacted with the oxidizing agent ($KMnO_4$) and then rinsed with $NaHCO_3$. The oxidized AC was then reacted with iron precursor ($FeSO_4.7H_2O$) to incorporate iron onto the surface of AC. Various molar compositions for mixing and preparing the iron modified ACs were followed and the resultant materials were labeled as B (0.1 M $KMnO_4$: 0.1 M $FeSO_4.7H_2O$), C (0.5 M $KMnO_4$: 0.1 M $FeSO_4.7H_2O$), D (0.1 M $KMnO_4$: 0.5 M $FeSO_4.7H_2O$) and E (1 M $KMnO_4$: 1 M $FeSO_4.7H_2O$). The selected samples were characterized by following techniques.

3.3 Scanning electron microscopy (SEM), transmission electron microscopy (TEM), high resolution TEM (HRTEM) and selected area electron diffraction (SAED)

The scanning electron microscope model Carl Zeiss Leo Supra 50 VP was used to examine the surface morphology (homogeneity/heterogeneity) of the powdered samples.

Likewise, TEM/HRTEM instrument model Phillips CM12 with Docu Version 3.2 80 kV equipped with a FEI TECNAI G2 Twin 200 kV field emission gun and Eagle camera was used to analyze in-depth surface texture of AC and FeACs. A volume of 10–30 mL from suspension of 5–10 mg powdered sample dissolved in 70% ethanol after ultrasonication was dropped on the copper grit and then analyzed under the microscope. However, HRTEM samples (after placing on the grit) were dried completely for whole day prior to analyses at a magnification up to 1.05 MHz. The lattice structure of the samples was investigated using SAED analyses.

3.4 Temperature programmed desorption (TPD) and temperature programmed reduction (TPR) studies

For all samples, TPR and TPD analyses were conducted to examine the presence of acidic or basic functional groups on solid samples. A Thermo-Finnigan TPD/R/O 1100 instrument carrying a thermal conductivity detector was used for TPR/TPD analyses. Prior to analysis, the undesired contents

were removed from the channel followed by refluxing sample with N_2 gas keeping flow rate 20 mL/min and ramp speed 10° C/min (ambient to 150° C). After degassing, the specimens were allowed to cooling and temperature was lowered down to 50° C. For TPR/TPD analyses, adsorbate gases (5 vol. % H_2 in Argon) and CO_2 at a flow speed 25 mL/min, ramp speed 10° C/min were allowed to adsorb/desorb on the samples in the temperature range of 50 to 900° C.

3.5 Iron impregnated ACs catalytic potential

Catalytic potential of iron impregnated ACs was examined by producing biodiesel using WCO as feedstock. The esterification and transesterification were proposed to be the major reactions involved. Initially, the WCO was sieved to remove any food debris followed by heating to remove water and other impurities. Afterwards, the mixture was allowed to settle down in a separating funnel. In the process of transesterification, pretreated oil with acid value (< 2) was taken. On the other hand, WCO (25 mL) heated up to 120° C was used in esterification process. Furthermore, methanol was added to it and stirred for 5 h at a stirring rate 600 rpm. Later on, acid catalysts, AC and FeACs reacted with WCO were finally treated with KOH. The solid catalyst was removed by allowing the mixture to settle down. The decanted product was transferred to a separating funnel to remove glycerol from biodiesel. The biodiesel produced was heated at 70° C to evaporate methanol contents. A pictorial form of fresh oil and WCO is depicted in Fig. 1.

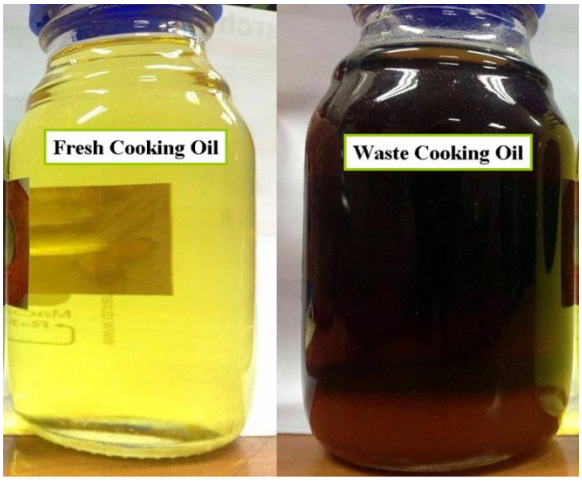

Fig. 1. An image of fresh cooking oil and WCO used.

4. RESULTS

4.1. SEM Analyses

The iron deposition impregnated AC was verified by SEM results. The changes in surface morphologies of AC and FeACs are depicted in Fig. 2. Smooth surface morphology with porous texture for AC whereas rough surface morphologies for FeACs were observed (Fig. 2). Similar results upon impregnation have been reported in literature [10]. The non-uniform aggregation of iron species on the surface and insides pores was found. The SEM image for sample E describes clearly the iron penetration into the pores, next to pores walls as well as upon the AC surface. With the changed surface morphology from uniform to irregular surface along with wider pores also depict the generation of extended porous structure, heterogeneity and formation of new active sites on the carbon matrix upon oxidization and Fe impregnation (Fig. 2).

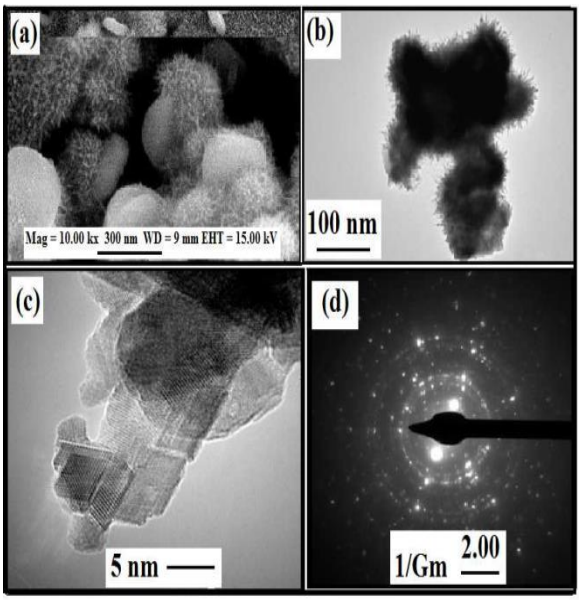

Fig. 2 (a) SEM, (b) TEM, (c) HRTEM and (d) SAED pattern for iron impregnated AC, sample E.

Upon oxidization more oxygen functional groups can be formed on AC surface. Furthermore, the iron impregnation of oxidized AC surface showed the Fe particles interaction with the oxygen moieties to form iron complexes. This leads to probable Fe particles penetration into the pores having pore size comparable to the dimensions of the iron species.

Hristovski et al. [11] also reported similar results for iron impregnated AC materials. The palette-like entities upon FeACs showed the iron incorporation into AC matrix. As mentioned above, it can be attributed to the formation of iron–oxygen complexes on FeACs.

4.2. TEM, HRTEM and SAED Analyses

The in-depth topography and layered structure of AC and FeACs were analyzed using TEM, HRTEM and SAED analyses. A slightly changed morphology of AC and E were observed (Fig. 2). These results also support SEM results and augment upon the surface roughness due to oxidization and Fe impregnation. Furthermore, the dendritic and rod shape texture of FeAC upon surface modification resulting in iron particles scattered inside and on the surface of AC can be clearly seen. An approximate diameter of the dendrite like structures (10 to 40 nm) was computed from the TEM images. The HRTEM images of the selected sample E is also depicted in Fig. 2. The image was captured at magnification of 1.09 Mx to investigate the iron impregnation impact on the layers arrangement of AC lattice. As can be seen in Fig. 2, the atomic layers are compact in E. This showed, iron impregnation can facilitate the layered arrangement of without using any templated system. It can be helpful for using FeACs in electrical applications.

The SAED pattern of E also described the polycrystalline arrangement of Fe incorporation into AC (Fig. 2). The XRD results in our recently reported work further support the SAED pattern, ring structure and particularly d-spacing [12]. In general, the incident beam's diffraction in x, y, z planes describes the existence of iron particles and correspondingly a crystalline texture in FeACs. In a closely relevant work, Filippousi et al., [13] reported magnetite and maghemite moieties derived from the indices (2 2 0), (3 1 1), (4 0 0), (4 2 2) and (5 1 1). On the other hand, SAED results for AC (not shown here) did not express the diffraction of light due to the absence of any metal atoms and non-crystalline character.

4.3. TPR-H_2 and TPD-CO_2 Results

TPR-H_2 results of AC and FeAC revealed the presence of oxygenated species by showing reduction peaks in their patterns (Fig. 3). The change in carrier gas (H_2) concentration was proportional to the surface reduction phenomenon over the surface of AC and FeACs.

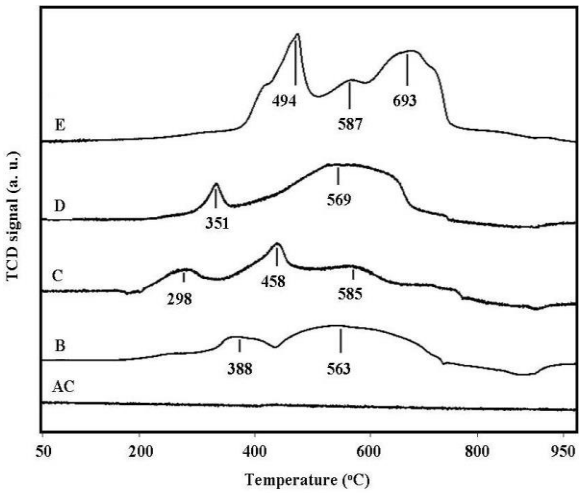

Fig. 3. H_2 TPR profiles of substrate AC and iron-modified activated carbons i.e. B, C, D and E.

As can be seen in Fig. 3, the reduction peaks of AC are very weak and almost disappeared since there were negligibly small amount of oxygen active groups. On the other hand, surface oxidization and Fe impregnation resulted in a large number of oxygen functionalities newly created upon the surface of FeAC which enhanced the H_2 consumption. Among all FeACs, E has shown the highest reduction values (Fig. 3). With the increase in temperature, the system may undergo through a transition state as well as reoxidation may occur. A good correlation of the results with the previously reported work commends on the surface modification [14]. From the TPR-H_2 results, it can be augmented that sample E can cope with catalytic character and can be potential catalyst.

The TPD-CO_2 profiles of AC and FeACs (Fig. 4) were used to demonstrate the presence of additional surface functional groups. It can be seen that, AC depict no desorption peak. Meanwhile, B, C, D and E profiles showed sharp and well defined desorption peaks. A few desorption peaks for sample E appearing at 670 and 741° C refers to significantly high values of CO_2 desorbed from its surface compared to all other FeACs samples. The decreasing trend of TPD-CO_2 values for the samples was as, E > D > C > B >> AC.

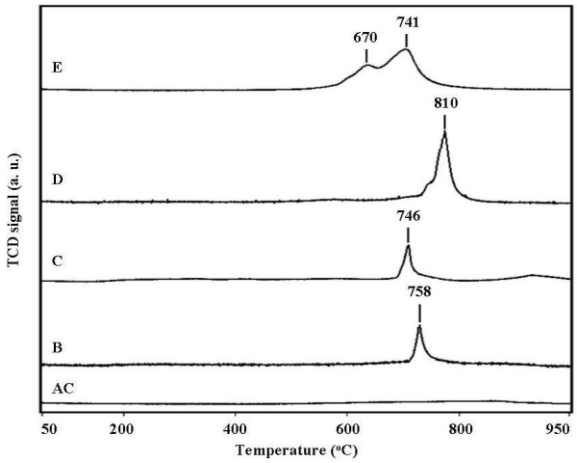

Fig. 4. TPD–CO_2 profiles of unmodified and iron-modified activated carbons i.e. B, C, D and E.

As can be seen in Fig. 4 that CO_2 desorption peaks were almost disappeared in AC's TPD profile whereas FeACs have shown several desorption peaks. The drastic change in the TPD-CO_2 profiles of AC and FeACs is preferably attributed to the surface modification of the substrate AC. It can be reinstate that surface oxidization and iron impregnation of AC resulted in the enlarged surface active sites created on the modified ACs with an increased amount of oxygen functionalities such as carboxyl, hydroxyl, carbonyl, lactones etc. which agrees with the previously reported literature as well [1]. Among all FeACs, sample E revealed with the highest values of CO_2 adsorption-desorption. It is expected that upon heating the oxidized surface, CO and CO_2 released due to the oxygenated groups e.g. carbonyls, ethers and phenols etc. decomposition. It is pertinent to mention that, carboxyl and lactones releases CO_2 at lower and higher temperatures, respectively [15].

TPD–CO_2 pattern of the materials can be split up in three regions i.e. weak, medium and strong regions depending upon the oxygen functionalities strength, active sites, bonding at the solid's surface and dispersion of metals on the surface [16]. Up to 400° C, the TPD profiles of AC and FeACs did not show any sharp desorption peak which can be correlated with the highly stable oxygen functional groups. However, FeACs exhibited sharp and well defined desorption peaks at temperatures above 700° C. The two characteristic peaks in TPD-CO_2 profile of E at 670 and 741° C (Fig. 4) are assignable to the decomposition of carbonylic and anhydride/ lactones groups, respectively [15], [17]. The characterization of AC and FeACs elaborate on the enhanced surface activity of E and the results are significantly supported by the TPD-CO_2 results. In addition to other improved physicochemical characteristics of the FeACs, the catalytic potential is also expected from these Fe modified samples.

4.4. WCO: Feedstock for biodiesel production

Fatty acid methyl ester (FAME) also named as biodiesel was attempted to be produced using a raw feedstock i.e. WCO in the presence of solid catalyst FeACs. In general, WCO consists of FFA that can be used to produce biodiesel. The major steps involved were esterification and transesterification of free fatty acids and triglyceride, respectively yet simultaneously. The selectivity of best acid catalyst among all materials is described in the following sections;

4.5. Optimization of reaction conditions and catalysts screening for biodiesel production

To validate the positive impact on the catalytic character of iron modified ACs, all materials including AC, B, C, D and E were tested for biodiesel production. In initial screening of the materials, conducting the same reaction run for three (3) times, the best material was chosen among all showing the highest FAME yield (%). Among all samples, E showed the highest catalytic potential in esterification of FFA and triglyceride transesterification yielding biodiesel and glycerol. Figure 5 shows the screening results of the best solid acid catalyst.

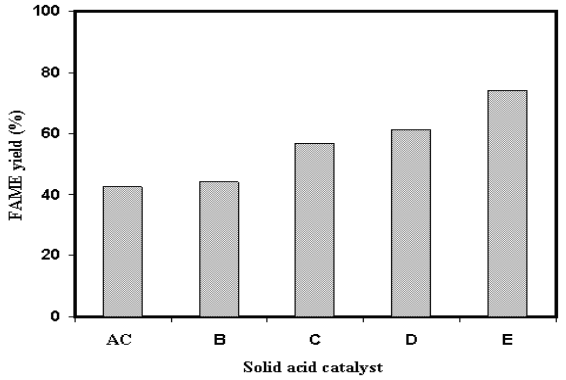

Fig. 5. Screening of solid catalysts for biodiesel production from WCO.

The major steps involved in biodiesel production are described as under (Fig. 6);

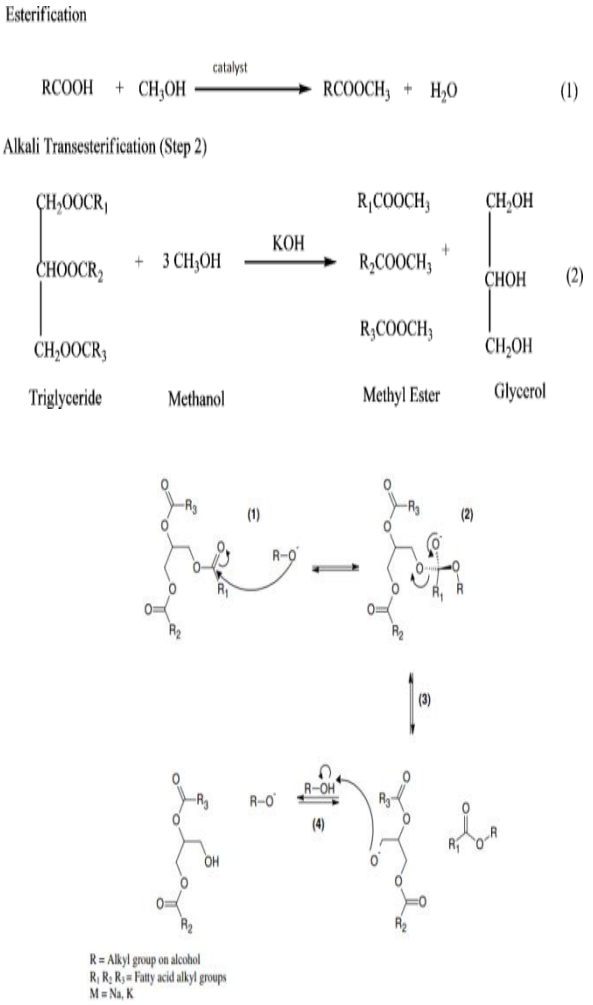

Fig. 6. Reaction mechanism involved in biodiesel production from WCO.

For confirmation of the biodiesel as major product of the reactions (Fig. 6), GC and FTIR studies were conducted. The GC profiles of standard with the FAME produced are depicted in Fig. 7 (a, b). As can be seen that, characteristic peaks in Fig. 7a (for standard) are also present in Fig. 7b (for FAME), which indicates the successful conversion of FFA into FAME. Thus, it is augmented that, raw feedstock WCO containing FFA were successfully converted into the fuel of present and future i.e. biodiesel using an acid catalyst, E, besides the presence of base catalyst, KOH. Initial screening of solid acid catalysts shown that, sample E yielded with the highest FAME values up to 75-78 %.

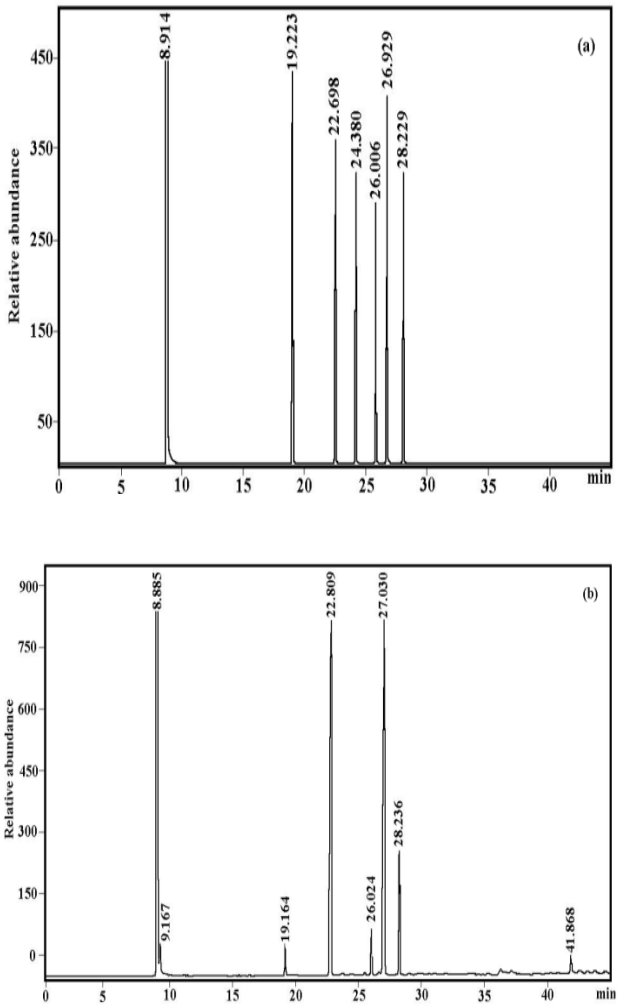

Fig. 7. GC-MS chromatograms of (a) standard and (b) biodiesel produced.

Table 1. Retention time of FAME present in the standard with biodiesel produced (T = 120 ^{o}C, t = 5 h, catalyst loading = 9 %, methanol/ WCO ratio, 1: 16).

FAME	Retention time (min)
Methyl myristate	19.223
Methyl palmitate	22.698
Heptadecanoate (IS)	24.38
Methyl stearate	26.006
Methyl oleate	26.929
Methyl linoleate	28.229

Moreover, in FTIR spectrum (Fig. 8), several peaks corresponding to the glycerol and ester groups can be seen which further proves the conversion of FFA into FAME via esterification and transesterification processes using acid catalyst, E.

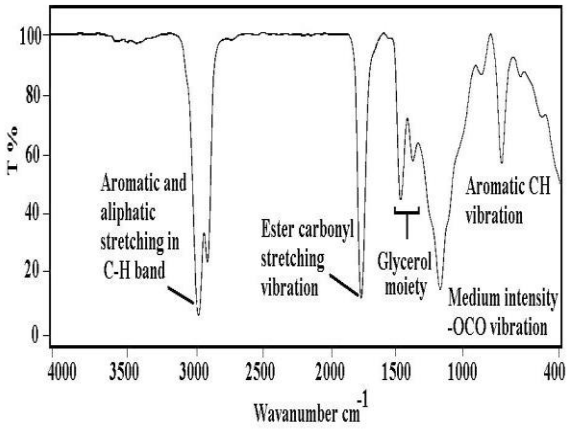

Fig. 8. The FTIR peaks distribution of biodiesel produced from WCO using solid acid catalyst (E) (T = 120 ^{o}C, t = 5 h, catalyst loading = 9 %, methanol to WCO ratio, 1: 16).

Figure 8 revealed with a number of peaks and shoulders for the biodiesel produced. A characteristic peak at 3000 cm^{-1} is attributable to the stretching of C-H band. Similarly, the peak appeared at 1750 cm^{-1} is associated with the stretching in ester and carbonyl linkages as were previously shown for the biodiesel obtained using palm oil as feedstock [18]. The peaks appearing at 1490 cm^{-1}can be correlated to the glycerol moieties. In addition, methyl propagation and/or medium intensity –OCO vibrations are advisable corresponding to the peaks at 1180 cm^{-1}. Moreover, the vibrating $(CH_2)_n$ group is abbreviated from the peaks found in region below 750 cm^{-1} is similar to a previous report as well [18].

The best acid catalyst after screening i.e. E, was further analyzed under the optimized conditions and has shown up to 78 % FAME yield. A comparison of FAME yields using various solid catalysts with the current work is tabulated in Table 2. In a closely related work, up to 94.8 % FAME was yielded at a sufficiently higher temperature (220 ^{o}C) in comparison to the current reaction temperature (i.e. 120 ^{o}C). Although, the FAME yield was high for Shu et al. [19] but the reaction conditions may not be practically appreciable. In another approach, Dawodu et al. [20], used carbonized solid catalysts but the FAME yield was too low i.e. 16.7 % and 11.5 % which seems not preferable to be adapted due to the low FAME yield. The current results, however, shows the enhanced utilization of otherwise inert adsorbent AC as a potential catalyst for biodiesel production using a raw feedstock at comparatively low temperature with sufficiently high FAME yield.

Table 2. A comparison of the reported literature with the current findings of biodiesel production.

Material used	FAME yield (%)	Reference
Carbonized vegetable oil asphalt	94.8	[19]
Carbonized defatted cake	16.7	[20]
Carbonized glucose	11.5	[20]
Iron impregnated AC (E)	78	This work

5. CONCLUSIONS

To enunciate the use of AC, it was successfully oxidized and impregnated with iron precursor via wet impregnation technique. An enhanced potential of all physicochemical characters with the advance application of FeACs was obtained. These changes were derived from the in-depth characterizations and additionally elaborating on the catalytic activity of the FeACs, particularly the sample E. The FeACs catalysts showed successful production of biodiesel from a raw feedstock, WCO. An approximately 78 % FAME yield in 5 h at 120^{o} C was observed at laboratory scale which can be further improved. This catalytic character adds more values to the otherwise inert AC materials which is important from the environmental as well as renewable energy perspectives and can be useful for practical applications.

NOMENCLATURE

WCO waste cooking oil

AC activated carbon

FeACs iron impregnated activated carbon materials

FAME	fatty acid methyl esters
FFA	free fatty acids
TPR	temperature programmed reduction
TPD	temperature programmed desorption
TEM	transmission electron microscopy
HRTEM	high resolution transmission electron microscopy
SAED	selected area electron diffraction
SEM	scanning electron microscopy
GC	gas chromatography
TCD	thermal conductivity detector
FTIR	Fourier transform infra-red spectroscopy
M	molar
MHz	mega hertz
mg	milligram
rpm	revolutions per minute
h	hour
kV	kilo volt
mL	milliliter
min	minute
nm	nanometer
cm^{-1}	per centimeter
^oC	degree Celsius

ACKNOWLEDGEMENTS

IS acknowledges the Higher Education Commission, Pakistan for awarding the funding as start-up research grant No: 21-1849/SRGP/R&D/HEC/2018 under the “Interim Placement of Fresh PhDs (IPFP)” program.

REFERENCES

[1] C. Y. Yin, M. K. Aroua, W. M. A. W. Daud, "Review of modifications of activated carbon for enhancing contaminant uptakes from aqueous solutions" *Separation and Purification Technology*, *52*, 403–415, 2007.

[2] M. Takase, M. Zhang, W. Feng, Y. Chen, T. Zhao, S. J. Cobbina, L. Yang, X. Wu, "Application of zirconia modified with KOH as heterogeneous solid base catalyst to new non-edible oil for biodiesel" *Energy Conversion and Management Journal*, 80, 117–125, 2014.

[3] S. Semwal, A. K. Arora, R. P. Badoni, D. K. Tuli, "Biodiesel production using heterogeneous catalysts" *Bioresource Technology*, 102, 2151-2161, 2011.

[4] J. R. Almeida, L. C. Fávaro, B. F. Quirino, "Biodiesel biorefinery: opportunities and challenges for microbial production of fuels and chemicals from glycerol waste" *Biotechnology and Biofuels*, 5, 48 (16 pg), 2012..

[5] J. L. Figueiredo and M. F. R. Pereira, "The role of surface chemistry in catalysis with carbons" *Catalysis Today*, 150, 2–7, 2010.

[6] L. J. Konwar, J. Boro, D. Deka, "Review on latest developments in biodiesel production using carbon-based catalysts" *Renewable and Sustainable Energy Reviews*, 29, 546–564, 2014.

[7] M. S. Khayoon and B. H. Hameed, "Acetylation of glycerol to biofuel additives over sulfated activated carbon catalyst" *Bioresource Technology*, 102, 9229–9235, 2011.

[8] K. Ngaosuwan, J. G. Goodwin, Jr., P. Prasertdham, "A green sulfonated carbon-based catalyst derived from coffee residue for esterification" *Renewable Energy*, 86, 262–269, 2016.

[9] Y.C. Brito, V. M. Mello, C. Cesar, C. S. Macedo, M. R. Meneghetti, A. Z. Suarez, S. M. P. Meneghetti, "Fatty acid methyl esters preparation in the presence of maltolate and

n-butoxide Ti(IV) and Zr(IV) complexes" *Applied Catalysis A: General*, 351, 24–28, 2008.

[10] C. Bouchelta, M. S. Medjram, O. Bertrand, J. P. Bellat, "Preparation and characterization of activated carbon from date stones by physical activation with steam" *Journal of Analytical and Applied Pyrolysis*, 82, 70–77, 2008.

[11] K. D. Hristovski, P. K. Westerhoff, J. C. Crittenden, L. W. Olson, "Arsenate removal by iron hydroxide modified granulated activated carbon: Modeling arsenate breakthrough with the pore surface diffusion model" *Separation Science and Technology*, 43, 3154–3167, 2008.

[12] I. Shah, R. Adnan, W. S. Wan Ngah, N. Mohamed, "Iron impregnated carbon materials with improved physicochemical characteristics" *Materials Science and Enginering B*, 201, 1-12, 2015.

[13] M. Filippousi, M. Angelakeris, M. Katsikini, E. Paloura, I. Efthimiopoulos, Y. J. Wang, D. Zamboulis, G. van Tendeloo, "Surfactant effects on the structural and magnetic properties of iron oxide nanoparticles" *Journal of Physical Chemistry C,* 118, 16209-16217, 2014.

[14] O. O. James, B. Chowdhury, S. Maity, "TPR and TPD studies of effects of Cu and Ca promotion on Fe–Zn-based Fischer– ropsch catalysts. *Journal of Chemical Sciences,* 125, 679–686, 2013.

[15] M. Vukcevic, A. Kalijadis, S. Dimitrijevic-Brankovic, Z. Lausevic, M. Lausevic, "Surface characteristics and antibacterial activity of a silver-doped carbon monolith" *Science and Technology of Advanced Materials*, 9, 015006 (7 pp), 2008).

[16] V. Dondur, V. Rakic, L. Damjanovic, A. Auroux, "Comparative study of the active sites in zeolites by different molecules" *Journal of The Serbian Chemical Society*, 70, 457–474, 2005.

[17] A. M. Kalijadis, M. M. Vukcevic, Z. M. Jovanovic, Z. V. Lausevic, M. D. Lausevic, "Characterisation of surface oxygen groups on different carbon materials by the Boehm method and temperature-programmed desorption" *Journal of the Serbian Chemical Society*, 76, 757–768, 2011.

[18] A. Ivanoiu, A. Schmidt, F. Peter, L. M. Rusnac, M. Ungurean, "Comparative study on biodiesel synthesis from different vegetables oils" *Chemistry Bulletin "POLITEHNICA"* University (Timisoara), 56, 94–98, 2011.

[19] Q. Shu, J. X. Gao, Z. Nawaz, Y. H. Liao, D. Z. Wang, J. F. Wang, "Synthesis of biodiesel from waste cooking oil with large amounts of free fatty acids using a carbon-based solid acid catalyst" *Applied Energy*, 87, 2589–2596, 2010.

[20] F. A. Dawodu, O. O. Ayodele, J. Y. Xin, S. J. Zhang, "Application of solid acid catalyst derived from low value biomass for a cheaper biodiesel production" *Journal of Chemical Technology and Biotechnology*, *89*, 1898–1909, 2014.

APPENDICES

Appendix A:

Characteristics of commercial AC received

Formula: C

Molecular weight: 12.01 g/mol

Packing size 500 g

Solubility in nitric acid: < 5.00 %

Solubility in water: < 2.00 %

Arsenic: < 0.0005 %

Lead: < 0.005 %

Iron: < 0.05 %

Zinc: < 0.01 %

n-hexane adsorption: > 25 %

Residue on ignition (at 600 ºC): < 5 %

Bulk density: 40 g/ 100 mL

Loss on drying: < 10 %